Title

Association of Placental Growth Factor and Angiopoietin in Human Retinal Endothelial Cell-Pericyte co-Cultures and iPSC-Derived Vascular Organoids.

Journal

Current Eye Research, 48(3)

Authors

Huang, Hu
Saddala, Madhu Sudhana
Mukwaya, Anthony
et al.

Publication Date

2023-03-01

DOI

10.1080/02713683.2022.2149808

Peer reviewed

HHS Public Access

Author manuscript

Curr Eye Res. Author manuscript; available in PMC 2024 March 01.

Published in final edited form as:

Curr Eye Res. 2023 March ; 48(3): 297–311. doi:10.1080/02713683.2022.2149808.

Association of placental growth factor and angiopoietin in human retinal endothelial cell-pericyte co-cultures and iPSC-derived vascular organoids

Hu Huang[a], **Madhu Sudhana Saddala**[a,b], **Anthony Mukwaya**[c,d], **Rajiv R. Mohan**[a], **Anton Lennikov**[e]

[a]Department of Ophthalmology, University of Missouri School of Medicine, Columbia, MO, USA

[b]Wilmer Bioinformatics, Johns Hopkins University School of Medicine, Baltimore, MD, USA

[c]Department of Ophthalmology, Institute for Clinical, and Experimental Medicine, Faculty of Health Sciences, Linköping University, Linköping, Sweden

[d]Department of Biochemistry and Molecular Biology, Faculty of Health Sciences, Busitema University, Uganda

[e]Department of Ophthalmology, Schepens Eye Research Institute of Massachusetts Eye and Ear, Harvard Medical School, Boston, Massachusetts, United States

Abstract

Purpose: Placental growth factor (PlGF) and Angiopoietin (Ang)-1 are two proteins that are involved in the regulation of endothelial cell (EC) growth and vasculature formation. In the retina and endothelial cells, pericytes are the major source of both molecules. The purpose of the present study is to examine the association of PlGF and Ang-1 with human EC/pericyte co-cultures and iPSC-derived vascular organoids

Materials and Methods: In this study, we used co-cultures of human primary retinal endothelial cells (HREC) and primary human retinal pericytes (HRP), as well as human-induced pluripotent stem cells (iPSC), derived organoids (VO) to study the association between PlGF and Ang-1, using western blotting, immunofluorescent analysis, TUNEL staining, LDH-assays and RNA seq analysis.

Corresponding Author: Hu Huang PhD, 1 Hospital Drive, MA102C, Columbia, MO 65212, Phone: +1 (573) 882-9899; huangh1@missouri.edu.

Author contributions: The study was conceived and designed by H.H.; H.H and AL performed in vitro experiments and evaluations. M.S.S. has performed RNA seq datasets analysis. M.S.S and H.H. have conducted DESeq2 and R program analysis, figure design, and statistical analysis. The manuscript was written by H.H., M.S.S, AM, RM and AL and critically revised by H.H., AM and AL. All authors reviewed and accepted the final version of the manuscript.

None of the authors has a conflict of interest with or source of funding for the submission.

Compliance with Ethical Standards: Not applicable

Conflict of interest: The authors report no conflicts of interest. The authors alone are responsible for the content and writing of the paper.

Animal Research: Not applicable

Informed consent: Not applicable

Results: Inhibition of PlGF by PlGF neutralizing antibody in HREC-HRP co-cultures resulted in the increased expression of Ang-1 and Tie-2 in a dose-dependent manner. This upregulation was not observed in HREC and HRP monocultures but only in co-cultures suggesting the association of pericytes and endothelial cells. Furthermore, Vascular endothelial growth factor receptor 1 (VEGFR1) inhibition abolished the Ang-1 and Tie-2 upregulation by PlGF inhibition. The pericyte viability in high glucose conditions was also reduced by VEGFR1 neutralization. Immunofluorescent analysis of VO Ang-1 and Ang-2 were expressed mainly by perivascular cells. RNA seq analysis of the RNA isolated from VO in high glucose conditions indicated increased P*l*GF and Ang-2 expressions in the VO. PlGF inhibition increased the expression of Ang-1 and Tie-2 in VO, increasing the pericyte coverage of the VO microvascular network.

Conclusion: Combined, these results suggest PlGF's role in the regulation of Ang-1 and Tie-2 expression through VEGFR1. These findings provide new insights into the neovascularization process in diabetic retinopathy and new targets for potential therapeutic intervention.

Keywords

PlGF; Angiopoietin; Tie 2; Diabetic retinopathy; Endothelial cell; Pericyte; RNA-seq; vascular organoids

Introduction

Diabetic retinopathy (DR) is the major vision-threatening complication of diabetes that dramatically decreases the quality of life of the affected patients.[1] As the visual cycle is an active source of oxidation in the retina, a balance change between oxidation and anti-oxidation mechanisms leads to diabetic retinopathy onset and progression.[2] The high glucose environment and insulin deficiency in the retina leads to increased oxidative stress, tissue hypoxia, chronic inflammation, microglia activation, and loss of retinal ganglion cells (RGC).[3,4] Microglia cell activation leads to constant retinal inflammation by production by producing proinflammatory cytokines such as Tumor necrosis factor-alpha (TNF-α), Interleukin-6 (IL-6), (C-C motif) ligand 2 (CCL-2; previously known as MCP-1).[5,6]. Early stages of non-proliferative DR (NPDR) involve various degrees of vascular abnormalities, including loss of pericytes, reduced blood-retinal barrier (BRB) function through the decrease of ZO-1 and Occludin-1, acellular capillaries, microaneurysms, retinal hemorrhages.[7,8] With the DR progression, these changes lead to reduced perfusion, retinal ischemia, and further loss of BRB. Clinically these changes in the retinal vasculature become noticeable in patients' fluorescent angiography (FA). [9] While the loss of ganglion cells remains largely unnoticed by the patient diabetic macular edema (DME) resulting from increased proinflammatory signaling and serum leakage into the retina dramatically reduces the patient's vision. The advancement of DR to the proliferative stage (PDR) is driven by increased production of proangiogenic factors such hypoxia-inducible factor-1 alpha (HIF-1α), vascular endothelial growth factor (VEGF), which drive microvascular endothelial cell proliferation, migration, angiogenic growth. Pathological neo-vasculatures grow across the inner limiting membrane into the retina and vitreous. These neo-vessels are fragile, leading to retinal and vitreal hemorrhages, eventually resulting in retinal detachment and loss of vision [1].

PlGF is the second member of the VEGF family of ligands cloned in 1991 (VEGF-A was discovered in 1989[10]).[11] PlGF is involved in pathological angiogenesis in a wide range of disease conditions, such as ischemia, inflammation and cancer, through the interaction with VEGF-A and its VEGFR1 (NRP1/NRP2) signaling.[12–15] The downstream molecules of the PlGF signaling pathway have been elucidated in detail.[16,17] PlGF's role in eye diseases has been extensively characterized.[18–22] Especially, PlGF was found to promote choroidal and retinal angiogenesis (retinal neovascularization) and is a potential therapeutic target to treat vasculopathies, such as wet AMD, PDR, and DME.[7,23–25] PlGF expression is increased in the vitreous in the DR/DME patients and the increase correlated with the disease severity.[22,26,27] PlGF, in addition to VEGF-A and VEGF-B, is directly targeted by the FDA-approved drug EYLEA® (Aflibercept), leading to a more superior therapeutic effect than treatments that target anti-VEGF (e.g., Ranibizumab, Bevacizumab) in the treatment of DME patients with worse baseline.[28] Angiopoietins are a class of secreted glycosylated peptides (i.e., Ang-1, Ang-2, Ang-, and Ang-4) that significantly regulate vascular integrity and quiescence in numerous inflammatory-related conditions. Ang-3 signaling is not well documented, while angiopoietins 1, 2, and 4 are ligands for the Tie-2 receptor [29], predominantly expressed by endothelial cells. It has been shown that Ang 1 signaling via Tie-2 maintains quiescence in the adult vascular endothelium [30].

Interestingly, Ang-2, a member of the angiopoietin family of glycosylated peptides, is widely believed to antagonize Ang-1 signaling. Despite the weak expression of Ang-2 by quiescent vascular endothelium, Ang-2 directly stimulates the phosphorylation of Tie-2. Ang-2 also destabilizes quiescent endothelium priming the vasculature to respond rapidly to exogenous stimuli such as inflammatory and angiogenic mediators. The central role of Ang-2 in regulating the rapid vascular response to stimuli is partly attributed to the ready-made, stored Ang-2 in Weibel–Palade bodies within endothelial cells [31], from where Ang-2 molecules are released quickly following stimulation to exert their effect. Functional studies indicated that Ang-2 affects pericyte coverage of the vasculum leading to BRB leakage and, thus, a potential therapeutic target for treating PDR and DME [32–34].

This study investigated a novel PlGF's/Ang-1/-2 and Tie-2 signaling axis *in vitro*, using human cell co-cultures, i.e., human retinal pericytes (HRP) and HREC, and blood vessel or vascular organoids (VO) derived from human induced pluripotent stem cells (iPSC). In line with this model system, we recently developed a three-dimensional (3D) human VO as a model for diabetic vasculopathy. This model showed similarities to human vasculatures as detailed elsewhere [35]. Pericyte coverage was examined using this model system in this study, and the relative expression and colocalization of PDGFRb relative to the endothelium were investigated. The goal was to provide insight into PlGF/VEGFR1 and Ang-1/Tie-2 signaling, with the knowledge generated serving as a basis for future therapeutic interventions for conditions affecting the back of the eye, such as DR, among others.

Materials and methods

Cell cultures and antibody treatments

The primary human retinal endothelial cells (HREC; Cat#: ACBR1 181) and human retinal pericytes (HRP; Cat#: ACBR1 183) were purchased from Cell Systems (Kirkland, WA)

and cultured based on the experimental procedures as described previously [36,37]. In brief, HREC were seeded on fibronectin-coated (1 μg/cm^2, Cat#: 1030-FN, R&D Systems). Plastic vessels and cultured with EBM2-MV medium (Cat#: cc-4176, Lonza) supplemented with EC growth factors (Cat#: cc-4147, Lonza). HRP cells were cultured with a complete pericyte culture medium (Cat#: 4N0-500, Cell Systems) with supplementation of normal glucose, culture boost (Cat#: 4CB-500, Cell Systems), and attachment factor (Cat#: 4Z0-201, Cell Systems). HREC and HRP cells were co-cultured at the ratio of 2:1 with the combination of two culture media. After HREC monolayer formation and HREC-HRP co-culture stabilization, the culture media were replaced with fresh ones with the following desired treatment agents: D-glucose (25 mM), mannitol (25 mM), hydrocortisone (50 mM), anti-P*l*GF antibody (PL5D11D4, Oxurion, Leuven, Belgium), and anti-VEGFR1 antibody (MF1, ImClone Systems). The treatment duration was 2 days. It is worth noting that the mouse anti-P*l*GF antibody was validated to bind with human P*l*GF protein in our previous study.[36] Both anti-P*l*GF and anti-VEGFR1 antibodies showed robust efficacy in *in-vivo* and *in-vitro* experiments. [23–25,38]

Human iPSC-derived vascular organoids cultures

Human iPSC cells reprogrammed from a non-disease human subject were obtained from Infinity BiologiX LLC, NJ (Subject: NDS00249; iPSC: ND50018; Passage 11). The iPSC cells were cultured and maintained with the mTeSR1 medium (Cat#: 85850, STEMCELL Technologies), which was formulated from basal medium (Cat#: 85851 STEMCELL) and supplement (Cat#: 85852, STEMCELL). Blood vessels or vascular organoids were generated according to the protocols described by Wimmer et al. [35,39]. Briefly, human iPSC cells were first aggregated on a 6-well low attachment plate with the mTeSR1 medium containing 50 μM Y27632 (ROCK inhibitor, Cat#: 688001, Calbiochem, Millipore/Sigma) for 1 day. Then, the iPSC cell aggregates were committed to mesoderm linage in the presence of 12 μM CHIR99021 (GSK3β inhibitor, Cat#: 4423, Tocris) and 30 ng/mL BMP-4 (Cat#: 78211, Stemcell Tech) for 3 days. The aggregated progenitor cells were further differentiated into vascular cells with 100 ng/ml VEGF-A and 100 ng/ml FGF-2 for 2 days. The final step was that vascular cells continue to sprout, grow and form a network in the collagen I-Matrigel matrix under the induction of VEGF-A and FGF-2 from 5 to 14 days. The success of vascular organoids was confirmed by 3-dimensional (3D) structures, vascular networks, and pericyte coverage.

P*l*GF enzyme-linked immunosorbent assay

The levels of P*l*GF in the culture supernatants were determined by the commercial P*l*GF enzyme-linked immunosorbent assay (ELISA) kit (DPG00, R&D Systems). The culture supernatants from HREC and HREC-HRP co-cultures were collected and filtered through Millex-GP Filter, 0.22 μm (LGPB5010, Sigma-Aldrich) to remove cells and cellular debris. The ELISA was performed according to manufacturer instructions using provided P*l*GF control standard curve. The resultant absorbances were read at 450 nm using an 800 TS Absorbance Reader (BioTek Instruments, Winooski, VT, USA).

Trans-endothelial electrical resistance measurement by an electrical cell-impedance sensing system

HRECs and HRP were seeded and co-cultured at a 2:1 ratio on the 8-well cultureware (PC, 8W10E). Trans-endothelial electrical resistance (TEER) changes were measured in real-time with the electrical cell-impedance sensing system (ECIS)-Zθ system (Applied Biophysics, NY). The ECIS software-embedded mathematical model of impedance change was used to calculate the TEER (Ω/cm^2), measuring the cell-cell barrier and cell-matrix resistance [40]. The single-frequency model (4000 Hz) measured resistance and impedance with a 300s interval. After the resistance stabilized and reached a platform, indicating the formation of confluent monolayer and functional barrier, The various treatments: IgG control, P*l*GF antibody (50 μg/ml), and P*l*GF antibody (50 μg/ml) + VEGFR1 antibody (50 μg/ml) was added to the medium and then continued to culture for two days. The normalized resistance values were expressed as a percentage relative to vehicle control.

Western blot and densitometric quantification

Western blot (WB) was performed according to the previously described methods with some modifications [24,36,41]. HREC and RRP were mono- and co-cultured to confluency in 6-well plates and used for WB analysis. In brief, the cells were washed with cold PBS three times, detached with a cell scraper, and collected by centrifugation. The harvested cell pellets were sonicated in cold RIPA buffer containing FAST protease inhibitors (Cat#: S8830, Sigma, St. Louis, MO). The protein concentration was determined with the DC™ Protein Assay kit (Bio-Rad) and Qubit 4 fluorometer.

Before the electrophoretic transfer to 0.45 μm pore-size nitrocellulose membranes, 30–50 μg total protein per lane were separated by 4–20% sodium dodecyl sulfate-polyacrylamide gel electrophoresis (SDS-PAGE). The membranes were blocked with 5% non-fat milk (Bio-Rad) or 2% BSA at room temperature for 1 hr and then incubated overnight at 4°C with the following primary antibodies (Table 1). After being washed with PBST buffer, the membranes were incubated with horseradish peroxidase (HRP)-conjugated secondary antibody (1:2000; Cell Signaling Technology) for 1hr at room temperature. Signals were developed with enhanced chemiluminescence with a SuperSignal West Pico kit (Thermo-Fisher) and detected with an ImageQuant LAS 500 (GE Healthcare).

RNA Isolation and Quantitative Real-Time PCR (qRT-PCR)

qRT-PCR was conducted accruing to the previously described protocol with some modifications[42]. Vascular organoids were washed with PBS, and total RNA was extracted using RNeasy Plus Mini Kit; (Qiagen) according to the kit protocol with the addition of RLT plus buffer supplemented with 20ul of 2M Dithiothreitol (DTT). RNA was analyzed for quality and quantified using a NanoDrop One (Thermo Fisher Scientific) and reverse transcribed to cDNA using Maxima™ H Minus cDNA Synthesis Master Mix, with dsDNase (M1682; Thermo Fisher Scientific), according to the manufacturer's protocol in SimpliAmp Thermal Cycler; (Life Technology, MA, USA). Gene expression analysis was performed using Power SYBR Green Master Mix (Thermo Fisher Scientific) with the following mouse-specific primers: (Table 2) in a Quant Studio 3 RT-PCR system (Applied Biosystems, CA, USA). The relative expression values of target genes were normalized to Cyclophilin as

the housekeeping gene, and the fold change was calculated using the relative quantification ($2^{-\Delta\Delta CT}$) method. Four biological replicates per treatment group were run in three technical replicates.

Immunofluorescence staining analysis

HRP cells and vascular organoids (VO) were cultured as described above. At the experiments' endpoints, the cells and VO samples were cryo-sectioned or flat-mounted, fixed in 4% paraformaldehyde (VVR Life Science), permeabilized by incubation in 0.05% Triton X-100, and blocked with 10% normal goat serum (NGS). The fixed samples were then incubated with the primary antibodies (Table 1). After washing with PBST buffer, the staining signals were visualized by goat anti-rabbit IgG (H + L) Cyanine5, goat anti-mouse IgG (H+L) Alexa Fluor 488, and goat anti-rat IgG (H+L) pacific blue. The non-specific staining and background tissue autofluorescence were established by incubating the sections of vascular organoids with secondary antibodies alone (Fig. S1). The cell nuclei were stained with DAPI (1:5,000). The slides were mounted with a ProLong Diamond antifade reagent (Thermo-Fisher) and imaged with an LSM 700 inverted laser confocal microscope (Carl Zeiss, Oberkochen, Germany).

TUNEL Assay for Detection of Apoptotic Nuclei

The terminal dUTP nick-end labeling (TUNEL) assay was performed according to previously described procedures with some modifications using the commercial kit (ApopTAG Red In Situ Apoptosis Detection Kit; Millipore, Temecula, CA) [6]. In brief, the cells were fixed in 1% paraformaldehyde for 10 minutes at room temperature and then washed twice for 5 minutes in PBS (pH7.4). After the tailing of digoxigenin-dNTP catalyzed by the TdT enzyme, the sections were incubated with the anti-digoxigenin-rhodamine antibody for 30 minutes at room temperature. The processed specimen was mounted with the antifade mounting medium for fluorescence-containing DAPI (Vectashield; Vector, Burlingame, CA) and viewed fluorescence microscope.

Cytotoxicity assay of the HRP cell cultures.

HRP cells were cultured in 96 well plates with normal glucose (5 mM D-glucose + 20 mM mannitol) and high glucose (25mM D-glucose) with or without anti-VEGFR1 antibody (50 μg/ml) for 5 days. MTT assay was performed to quantitively evaluate the cell viability caused by high glucose and anti-VEGFR1 ab. The resultant absorbances were read at 570 nm using an 800 TS Absorbance Reader (BioTek Instruments, Winooski, VT, USA).

Colocalization analysis of the double-stained vascular organoids

The vascular organoids treated IgG control, and P*/*GF ab was immuno-stained with the primary antibodies against EC marker CD31 and pericyte marker PDGFRb and the secondary goat anti-rabbit IgG (H + L) Cyanine5, goat anti-mouse IgG (H+L) Alexa Fluor 488. Immunofluorescence images were taken with EVOS M7000 fluorescent microscopy. ImageJ software analyzed the colocalization correlation between green and red signals by the JACoP (Just Another Co-localization Plugin) plugin. Briefly, after being imported into ImageJ software, the two channels were converted to 8-bit for analysis. Then, the

JACoP plugin was used for colocalization analysis between two channels (green and red), followed by an online document (https://imagej.nih.gov/ij/plugins/track/jacop2.html). Pearson's correlation coefficient and Manders' Coefficients (M1 & M2 overlay coefficients) with Costes' automatic threshold in the result panels were used for further statistical analysis.

Bioinformatics analysis of RNA sequencing data

RNA-Sequencing raw data was downloaded from the Sequencing Read Archive (SRA), which is available at: https://www.ncbi.nlm.nih.gov/sra/?term=SRP092491, which data was originally produced by Wimmer et al. 2019 and deposited in SRA (Bioproject: PRJNA352279) [35]. In summary, iPS cells were differentiated into vascular organoids and treated for 3 weeks with a diabetic media containing 75mM Glucose, 1ng/mL TNF-α, 1ng/mL IL6 (DI) or were untreated in 17mM Glucose (NG). The endothelial cells were sorted by FACS using CD31 as the marker. CD31 and sorted cells were stored at 80°C until use. The two NG (Normal Glucose) and 2 DI (Diabetes Induced) are pools of sorted endothelial cells from multiple vascular organoids (>100) from 2 independent differentiations/treatments.

Raw reads were mapped to the genome (hg19) using HISAT2 0.1.6[43]. Only reads with unique mapping were considered for further analysis. Gene expression levels were calculated using the HISAT2 software package (http://daehwankimlab.github.io/hisat2/). Normalization and differential expression analysis were done using the DESeq2 R package (Bioconductor, https://bioconductor.org/packages/release/bioc/html/DESeq2.html). Differentially expressed genes were selected using a twofold change cut-off between at least two populations, and $P < 0.05$ was adjusted for multiple gene testing. The Gene expression matrix was clustered using a k-means algorithm with correlation as the distance metric.

Statistical Analysis

The values were expressed as the mean ± standard deviation (SD) for the respective groups. Statistical analyses were performed with GraphPad Prism 8 software. Analysis of variance (ANOVA) or a linear mixed model was used for the statistical comparisons of multiple groups [44]. The *p*-values were adjusted for multiple comparisons with Dunnett's test. The non-parametric Mann–Whitney U test was performed to determine the significance level between the two groups. Statistical significance was set at $p < 0.05$.

Results

P*l*GF blockade regulates Ang-1 and Tie-2 in HREC-HRP co-cultures in an antibody concentration-dependent manner

To investigate whether P*l*GF is involved in pericyte-endothelial cross-talks, we first examined the PlGF level in HREC culture and HREC-HRP co-culture media. The PlGF level was 32.6 ± 2.8 pg/ml in the HREC cultures and 46.5 ± 3.7 pg/ml in the co-cultures. Next, we investigated the effect of P*l*GF blockade on the expression levels of Ang-1, Tie-2, VE-Cadherin, and N-Cadherin proteins in the HREC-HRP co-cultures. The confluent co-cultures were treated with the neutralizing P*l*GF antibody (PL5D11D4) at

three concentrations (25, 50, and 100 μg/ml) for two days. WB analysis was performed to examine the protein expression changes. WB barely detected Tie-2 protein expression in the vehicle control samples (Fig. 1A). The P*l*GF antibody at the dose of 25 μg/ml slightly increased the Tie-2 protein level compared with vehicle control. 50 and 100 μg/ml antibody doses up-regulated the Tie-2 protein expression compared with vehicle control and 25 μg/ml antibody. WB detected N-Cadherin, VE-Cadherin, and Ang-1 protein expressions in all four groups (Fig. 1A, B). 25 μg/ml P*l*GF antibody decreased the protein abundance of N-Cadherin (N-Cad) and Ang-1 but not VE-Cadherin (VE-Cad) compared with vehicle control. 50 and 100 μg/ml P*l*GF antibody concentrations up-regulated protein levels of Ang-1 but not N-Cad or VE-Cad compared with control and 25 μg/ml antibody. The protein blots were quantified to determine whether there were significant differences between treatment groups. The quantitative results (Fig. 1C, D) revealed no significant differences for Tie-2 between vehicle control and 25 μg/ml antibody, between 50 and 100 μg/ml P*l*GF antibody. However, the two higher antibody doses (50 and 100 μg/ml) significantly up-regulated Tie-2 protein expression compared with the lower antibody dose (25 μg/ml) and control conditions. 25 μg/ml P*l*GF antibody downregulated N-cadherin compared with vehicle control. There were no significant differences for VE-cadherin between any groups. 25 μg/ml antibody downregulated, but the two higher doses up-regulated Ang-1 compared with vehicle control. These results indicate that P*l*GF regulates the protein expressions of Ang-1 and Tie-2 but not N-Cad or VE-Cad depending on antibody concentration.

Ang-1 upregulation by P*l*GF blockade in HREC-HRP co-cultures, but not monocultures

It is well established that Ang-1 is secreted by the peri-endothelial cells, such as pericytes, and regulates Tie-2 signaling activity in endothelial cells in a paracrine manner [45]. Therefore, we examined whether the upregulation of Ang-1 protein expression by P*l*GF blockade requires HREC-HRP cross-talks. The confluent HREC, HRP mono- and co-cultures were treated with 50 μg/ml P*l*GF antibody for two days (the effective dose from above). The western blots detected Ang-1 protein expression in all three cultures: HRP monoculture, HREC monoculture, and HRP-HREC co-cultures (Fig. 2A–C). P*l*GF antibody up-regulated Ang-1 protein expression in the HRP-HREC co-cultures but not the two monocultures compared to vehicle control. Densitometry analysis of protein blots confirmed a significant difference between the P*l*GF antibody and IgG control in the co-cultures but not the monocultures (Fig. 2D–F). We also examined the expression of the Ang-2 protein (a partial agonist/antagonist of Tie-2) and the effect of P*l*GF inhibition in the three culture systems. Ang-2 expression was detected in the HRP-HREC co-cultures and HRP monocultures. However, WB failed to detect Ang-2 expression in HREC monocultures. Because that ECs could express and store Ang-2 [46], we should be cautious about interpreting this result, possibly caused by the expression level of Ang-2 that is not enough for the immunoblotting to detect in the cultured HRECs. Compared with vehicle control, WB and densitometry analyses revealed that P*l*GF inhibition does not alter Ang-2 protein expression in all three culture systems. These results indicate that Ang-1 upregulation by P*l*GF blockade is dependent on EC-pericytes cross-talk, and the relative ratio of Ang-1 to Ang-2 was increased due to the Ang-1 upregulation and Ang-2 non-alteration, which may contribute to the beneficiary effect of P*l*GF blockade on EC integrity and function, as we reported previously [36].

VEGFR1 is involved in P*l*GF's effect on Ang-1 and Tie-2 expression and EC barrier function

P*l*GF confers function (i) directly through VEGFR1, (ii) through heterodimerizing with VEGF-A and activation of VEGFR1 and R2, or (iii) through replacing VEGF-A from VEGFR1 to VEGFR2, then indirectly activating VEGF-A/VEGFR2 signaling. We asked what mechanism through which P*l*GF regulates Tie-2 and Ang-1 gene expression and EC barrier function. First, we found that VEGFR1 inhibition reduced the increased Tie-2 and Ang-1 protein levels caused by P*l*GF blockade compared to the vehicle control, suggesting that VEGFR1 is involved in the expression regulation (Fig. 3A, B). VEGFR1 inhibition also reduced EC barrier function, as indicated by reduced resistance (Fig. 3C). Since VEGFR1 inhibition antagonizes the effects of P*l*GF blockade, it is unlikely that P*l*GF exerts this function directly via VEGFR1 or heterodimerizing with VEGF-A and activating both VEGFR1 and R2 receptors. Therefore, it is reasonable to infer that P*l*GF blockade up-regulates Ang-1 and Tie-2 expression and promotes EC barrier function indirectly through activating VEGF-A/VEGFR1 signaling: P*l*GF blockade makes more VEGFR1 available to VEGF-A; thus, VEGFR1 blockade attenuates P*l*GF's promoting effect on gene expression and barrier function. Notably, the combination of anti-PlGF and anti-VEGFR1 did not reduce the levels of Tie2 and Ang-1 and the resistance back to baseline, suggesting that other factors are involved in the effect of PlGF inhibition.

VEGFR1 inhibition reduces pericyte viability in high-glucose conditions

We investigated whether VEGFR1 mediates pericytes viability in cell cultures in high glucose (HG, diabetes-like) conditions. HG treatment reduced viability, as shown by LDH and MTT results (Fig. 4A, B). Apoptotic cells were significantly increased in HG + VEGFR1 inhibition conditions than in normal glucose control and HG condition (Fig. 4C), indicating VEGFR1's involvement in pericyte survival. Additionally, by using an anti-phospho-(p)VEGFR1 antibody, we found that the phosphorylated or activated VEGFR1 form was co-localized with the apoptotic cells (either Caspase 3^+ or $TUNEL^+$) induced by HG (Fig. 4D–F).

iPSC-derived vascular organoids

Blood vessels or vascular organoids have recently been created from human ESC and iPSC as an appealing model for diabetic vasculopathy [35,39] We have successfully generated 3-dimensional (3D)-VO from human iPSC, which are structurally and functionally similar to human vasculatures and contain the key vascular components, including CD 31 (+) EC-formed vessel lumen structures, the associated PDGFRb (+) pericytes, and the Col IV (+) basements deposits Fig. 5 (A–C) [47] The results of whole mount stainings were further confirmed in immunostaining in cryosections (Fig. S1). The 3D reconstruction of CD31 staining deep z-stack images has revealed complex vascular meshwork within the organoid (Fig. 5D).

Upregulation of P*l*GF and Ang-2 by the diabetes-mimicking condition in vascular organoids

Using the RNA sequencing data of the VO treated with diabetes-like conditions versus normal medium available from the public database [35], we performed bioinformatics data

analysis. The results revealed that both P*l*GF and Ang-2 were significantly up-regulated in the diabetes-mimicking treatment group compared to the control group (Fig. 6A–C). Then, we examined their expression in the VO using double immunofluorescence staining. The results revealed that P*l*GF and Ang-2 were expressed in perivascular cells associated with $CD31^+$ ECs (Fig. 6D–I). The double stain of P*l*GF and Ang-2 showed the two proteins had similar but not identical expression patterns (Fig. 6J–L), indicative of heterogenous peri-vascular cell types, such as pericytes, smooth muscle cells, and others.

P*l*GF blockade up-regulates Ang-1 and Tie-2 in human iPSC-derived vascular organoids

We further examined whether the P*l*GF blockade could up-regulate Ang-1 and Tie-2 in human iPSC-derived vascular organoids; as P*l*GF antibody at 50 μg/ml for 2 days was effective in the human EC-pericyte co-cultures, we, therefore, doubled the antibody amount and treatment duration (100 μg/ml, 4 days) for the vascular organoids. The treated vascular organoids were cryosectioned for the double immunofluorescence staining analysis of Tie-2 and Ang-1. The results showed the increased staining signal intensity in the P*l*GF ab treatment group compared with the IgG control (Fig. 7 A, B).

The quantification of staining intensity revealed the increased Ang-1 and Tie-2 expression levels by P*l*GF ab treatment compared to the vehicle control (Fig. 7 C). qPCR further confirmed that the mRNA transcripts of Ang-2 and Tie-2 were up-regulated in the antibody treatment relative to the control (Fig. 7 D).

P*l*GF blockade promotes pericyte coverage and EC-pericyte association in vascular organoids

Finally, we investigated whether P*l*GF blockade promotes pericyte coverage and pericyte-EC association in vascular organoids, which was evaluated by the expression levels and correlation coefficiency of the PDGFRb's staining signal relative to the CD31's. The two-channel images have been calculated for relative expression and colocalization: the green channel for pericytes and the red channel for ECs (Fig. 8A–C, Fig S3). We used Image J with the JACop plugin to calculate Manders' overlap coefficient, which indicates the co-relations of the green (M1) and the red (M2). The M1 value for the green channel is 0.59 ± 0.5, and the M2 value for the red channel is 0.99 ± 0.0006 in control. The M1 is 0.89 ± 0.13, and the M2 is 0.99 ± 0.0017 in PlGF-ab treated group (Fig. 8D). As indicated by the cytofluorogram (Fig. 8E, F), P*l*GF ab treatment caused an increased Pearson's correlation coefficient of green signals versus red signals, which indicates that the P*l*GF blockade leads to increased coverage and colocalization of pericytes and ECs on organoid vasculatures.

Discussion

The present study described primary findings include 1) P*l*GF blockade up-regulates Tie-2 and Ang-2 expression in both HREC-HRP co-culture and human iPSC-derived vascular organoids, 2) VEGFR1 is involved in P*l*GF's regulation of Tie-2 and Ang-2 expression, 3) VEGFR1 inhibition reduces pericyte cell viability in high glucose condition, 4) P*l*GF and Ang-2 are expressed in perivascular cells and up-regulated by diabetes-mimicking conditions in the VO, and 5) P*l*GF blockade promotes pericyte coverage and association

with ECs in the VO. This study is the first to illustrate the direct regulation of the two signaling axis in human retinal cells and VO vasculatures. The data highlight P*l*GF's regulation of Ang-1 and Tie-2 in human cells and vascular organoids. The significance of the two signaling pathway regulations is relevant to stabilizing the endothelium facilitating vascular function by enhancing pericyte coverage and association with ECs.

Although angiopoietins are thought to directly affect cell adhesion by interacting with integrins, the expression of N-Cadherin in this study was not altered by the P*l*GF blockade. Alternative and compensatory regulatory mechanisms may be responsible for this observation which is in line with previous reports on the same [48]. P*l*GF inhibition by the varying antibody concentrations affects the regulation of Ang-1 and Tie-2 gene expression. Inhibition of PlGF at antibody doses of 50 and 100 μg/ml led to increased expression of Ang-1 and Tie-2, which signaling axis is important for EC-pericyte cross-talk and vascular stability. Lower antibody inhibition (i.e., 25 μg/ml) of PlGF reduces N-Cadherin expression. N-Cadherin is highly expressed in mesenchymal cells, thus a marker of the EC to mesenchymal transition (EndMT) [49,50] and epithelial-to-mesenchymal (EMT) [51,52] Therefore, this result suggests that P*l*GF inhibition at a low level might be involved in reducing EndMT. [49–52] The difference between PlGF antibodies at low and high doses might reflect that the degree of PlGF inhibition has a different effect on endothelial cell function: EndMT reduction requires less N-Cadherin and Ang-1, while vascular stability needs more Ang-1 and Tie-2. The observation that upregulation of Ang-1 occurred only in HREC-HRP co-culture but not monoculture suggests that a positive feedback loop may exist between pericytes and ECs. For example, the secreted pericyte Ang-1 activates Tie-2 in the ECs; subsequently, the activated Tie-2 triggers the signaling cascades in the ECs that up-regulate Ang-1 expression in the pericytes. These findings agree with our previous *in-vivo* study showing that P*gf* gene knockout prevents diabetes-caused pericyte loss and up-regulates Ang-1 expression in the retina using diabetic P*l*GF knockout (Akita.P*l*GF$^{-/-}$) mice. [7] Despite Ang-2 (the antagonist of Ang-1) not being changed in our experimental settings (50 μg/ml PlGF dose and 1:1 ratio of EC/pericyte), we could not rule out that PlGF inhibition regulates Ang-2 expression under other experimental conditions.

To further confirm the regulatory mechanism observed in 2D co-cultures of human retinal EC and pericytes, we exploited 3D vascular organoid cultures derived from human iPSC. As shown in Fig. 5, vascular organoids contain critical vascular components similar to human vasculatures, including the lumen-forming ECs, the closely associated pericytes, and the deposited basements, similar to those described by Wimmer et al. [35,47] Vascular organoids are physiologically similar to the *in-vivo* vascular organs more than the traditional 2D cell cultures, representing a new attractive model system to study vascular physiology and screen new drugs for vasculopathy. Moreover, iPSC can be derived from human patients, which renders the patient-derived vascular organoids (PDVO) powerful tools to mimic vascular diseases, screen drugs, and design personalized or precision medicine to treat vascular diseases, such as cardiovascular diseases, diabetic complications, and ischemic stroke. We used human iPSC-derived vascular organoids in the present study to evaluate the pericyte-endothelial cross-talk by P*l*GF and Ang signaling pathways. Furthermore, we performed transcriptome bioinformatic analysis for the RNA sequencing data from the blood vessel organoids treated with diabetic conditions (high glucose + TNF-alpha + IL-6) versus vehicle

control [35]. The results revealed that both PlGF and Ang-2 are significantly up-regulated in the blood vessel organoids by diabetic conditions.

It is well documented that Ang mediates its effects via Tie-2, maintaining quiescence in the adult vascular endothelium [30] and that VEGF is the main angiogenic cue molecule. Given the well-known limitations of the current mono anti-VEGF treatments, alternative treatment targets and treatment approaches have been on the agenda of many preclinical and clinical research groups. An example is combinational treatments, which involve targeting at once two or more molecules involved in the pathophysiology of a condition. In line with this, ongoing combinational therapy trials modulate both Ang-2 and the VEGF signaling to generate healthy, properly formed neovessels rather than pathological leaky neovessels[53,54]. Also, modulation of PlGF and Ang (Ang-1 and Ang-2) is an attractive therapeutic target for treating DR and DME[55,56].

Given the importance of Ang-1 in the pathophysiology of DR, our results provide novel and important insight into the Ang-1 signaling axis involving PlGF-VEGFR1 signaling. Interestingly, In support of the combinational treatment strategy and in support of the idea of therapeutically targeting PIGF, two large-scale phases 3 clinical trials (NCT03622580 and NCT03622593) were carried out to evaluate the bispecific molecule (Faricimab), which targets VEGF-A and Ang-2, for the treatment of wet age-related macular degeneration (AMD) and DME, in comparison to Aflibercept which targets VEGF-A and PlGF. These trials lead to the recent approval of Faricimab for the treatment of nvAMD and DME in the US[57]. In line with the importance of PIGF signaling, two phase-2 clinical trials (NCT03071068 and NCT03499223) have completed the safety and efficacy of a humanized PlGF antibody (THR-317) in the treatment of DR and DME. [36,37] However, no significant improvement was observed in Best Corrected Visual Acuity (BCVA) with the combination therapy THR-317 and ranibizumab compared to ranibizumab monotherapy in the overall study population. The combination therapy showed improvement in patients with poor or no response to prior anti-VEGF agents and patients with baseline BCVA ≤6 letters. [58] However, the funding of further clinical trials of THR-317 was discontinued in 2019, as the company chose to focus resources on other DR and DME therapeutic agents.

The present study investigated PlGF's regulation of the Ang-1 and Ang-2 expression in the HREC-HRP co-cultures and the vascular organoids derived from human iPSC. Herein, we provided evidence suggesting that PlGF blockade enhances EC-pericyte cross-talk by controlling the Ang-1/Tie-2 signaling axis. VEGFR1 acts as one downstream molecule of PlGF signaling to mediate cell viability and Ang-1 expression in the pericyte.[59]

The present study includes several limitations.

1. We characterized the levels of PlGF and PlGF-VEGF dimers in the supernatants of HREC cultures [36] but did not characterize their levels in HREC-HRP co-cultures and vascular organoids.
2. We evaluated the levels of Ang1 and Ang2 in cell lysates, but not the secreted proteins level is needed as low intracellular levels may be explained by increased secretion of the protein.

3. We only tested the effect of VEGFR1 inhibition, but not the effect of anti-PlGF Ab (PL5D11D4) or a combination of both Abs on the Ang2 and Tie2 levels.
4. We were unable to perform the immunoprecipitation or proximity ligation assay to confirm the physical interaction of PlGF and Ang-1.

Conclusion

The present study provides new evidence for the association of PlGF and angiopoietin in human retinal EC-pericyte co-cultures and iPSC-derived vascular organoids. The outcomes are relevant to diabetic retinopathy and other vascular pathophysiology. Further investigations are needed to elucidate the regulatory mechanisms further and promote translational potentials by targeting PlGF and Ang-1 signaling pathways.

Supplementary Material

Refer to Web version on PubMed Central for supplementary material.

Acknowledgments

The authors like to acknowledge the contributions of a lab technician Ms. Lijuan Fan for assistance with iPSC-derived vascular organoid cultures.

Funding:

This work was supported by NIH R01 grant (EY027824, H.H.), Missouri University start-up fund (H.H.) and Missouri University Postdoctoral Research Grant (A.L.).

Data availability statement

The authors confirm that the data supporting the findings of this study are available within the article and its supplementary materials. RNA-Sequencing raw data (Bioproject: PRJNA352279) originally produced by Wimmer et al. 2019 is available at: https://www.ncbi.nlm.nih.gov/sra/?term=SRP092491

References

1. Antonetti DA, Klein R, Gardner TW. Diabetic retinopathy. N Engl J Med 2012;366(13): 1227–39. [PubMed: 22455417]
2. Du Y, Veenstra A, Palczewski K, Kern TS. Photoreceptor cells are major contributors to diabetes-induced oxidative stress and local inflammation in the retina. Proc Natl Acad Sci U S A 2013;110(41):16586–91. [PubMed: 24067647]
3. Ghirlanda G, Di Leo MA, Caputo S, Cercone S, Greco AV. From functional to microvascular abnormalities in early diabetic retinopathy. Diabetes Metab Rev 1997;13(1):15–35. [PubMed: 9134346]
4. Barber AJ, Baccouche B. Neurodegeneration in diabetic retinopathy: Potential for novel therapies. Vision Res 2017;139:82–92. [PubMed: 28988945]
5. Miller WP, Yang C, Mihailescu ML, Moore JA, Dai W, Barber AJ, Dennis MD. Deletion of the Akt/mTORC1 Repressor REDD1 Prevents Visual Dysfunction in a Rodent Model of Type 1 Diabetes. Diabetes 2018;67(1):110–119. [PubMed: 29074598]

6. Huang H, Gandhi JK, Zhong X, Wei Y, Gong J, Duh EJ, Vinores SA. TNFalpha is required for late BRB breakdown in diabetic retinopathy, and its inhibition prevents leukostasis and protects vessels and neurons from apoptosis. Invest Ophthalmol Vis Sci 2011;52(3):1336–44. [PubMed: 21212173]
7. Huang H, He J, Johnson D, Wei Y, Liu Y, Wang S, Lutty GA, Duh EJ, Semba RD. Deletion of placental growth factor prevents diabetic retinopathy and is associated with Akt activation and HIF1alpha-VEGF pathway inhibition. Diabetes 2015;64(1):200–12. [PubMed: 25187372]
8. Hu J, Dziumbla S, Lin J, Bibli SI, Zukunft S, de Mos J, Awwad K, Fromel T, Jungmann A, Devraj K and others. Inhibition of soluble epoxide hydrolase prevents diabetic retinopathy. Nature 2017;552(7684):248–252. [PubMed: 29211719]
9. Duh EJ, Sun JK, Stitt AW. Diabetic retinopathy: current understanding, mechanisms, and treatment strategies. JCI Insight 2017;2(14).
10. Leung DW, Cachianes G, Kuang WJ, Goeddel DV, Ferrara N. Vascular endothelial growth factor is a secreted angiogenic mitogen. Science 1989;246(4935):1306–9. [PubMed: 2479986]
11. Maglione D, Guerriero V, Viglietto G, Delli-Bovi P, Persico MG. Isolation of a human placenta cDNA coding for a protein related to the vascular permeability factor. Proc Natl Acad Sci U S A 1991;88(20):9267–71. [PubMed: 1924389]
12. Fischer C, Jonckx B, Mazzone M, Zacchigna S, Loges S, Pattarini L, Chorianopoulos E, Liesenborghs L, Koch M, De Mol M and others. Anti-PlGF inhibits growth of VEGF(R)-inhibitor-resistant tumors without affecting healthy vessels. Cell 2007;131(3):463–75. [PubMed: 17981115]
13. Cao Y, Linden P, Shima D, Browne F, Folkman J. In vivo angiogenic activity and hypoxia induction of heterodimers of placenta growth factor/vascular endothelial growth factor. J Clin Invest 1996;98(11):2507–11. [PubMed: 8958213]
14. Uemura A, Fruttiger M, D'Amore PA, De Falco S, Joussen AM, Sennlaub F, Brunck LR, Johnson KT, Lambrou GN, Rittenhouse KD and others. VEGFR1 signaling in retinal angiogenesis and microinflammation. Prog Retin Eye Res 2021;84:100954. [PubMed: 33640465]
15. Snuderl M, Batista A, Kirkpatrick ND, Ruiz de Almodovar C, Riedemann L, Walsh EC, Anolik R, Huang Y, Martin JD, Kamoun W and others. Targeting placental growth factor/neuropilin 1 pathway inhibits growth and spread of medulloblastoma. Cell 2013;152(5):1065–76. [PubMed: 23452854]
16. Jiao W, Ji JF, Xu W, Bu W, Zheng Y, Ma A, Zhao B, Fan Q. Distinct downstream signaling and the roles of VEGF and PlGF in high glucose-mediated injuries of human retinal endothelial cells in culture. Sci Rep 2019;9(1):15339. [PubMed: 31653890]
17. Sissaoui S, Egginton S, Ting L, Ahmed A, Hewett PW. Hyperglycaemia up-regulates placental growth factor (PlGF) expression and secretion in endothelial cells via suppression of PI3 kinase-Akt signalling and activation of FOXO1. Sci Rep 2021;11(1):16344. [PubMed: 34381074]
18. Nguyen QD, De Falco S, Behar-Cohen F, Lam WC, Li X, Reichhart N, Ricci F, Pluim J, Li WW. Placental growth factor and its potential role in diabetic retinopathy and other ocular neovascular diseases. Acta Ophthalmol 2018;96(1):e1–e9. [PubMed: 27874278]
19. Van Bergen T, Etienne I, Cunningham F, Moons L, Schlingemann RO, Feyen JHM, Stitt AW. The role of placental growth factor (PlGF) and its receptor system in retinal vascular diseases. Prog Retin Eye Res 2019;69:116–136. [PubMed: 30385175]
20. Miyamoto N, de Kozak Y, Jeanny JC, Glotin A, Mascarelli F, Massin P, BenEzra D, Behar-Cohen F. Placental growth factor-1 and epithelial haemato-retinal barrier breakdown: potential implication in the pathogenesis of diabetic retinopathy. Diabetologia 2007;50(2):461–70. [PubMed: 17187248]
21. Kowalczuk L, Touchard E, Omri S, Jonet L, Klein C, Valamanes F, Berdugo M, Bigey P, Massin P, Jeanny JC and others. Placental growth factor contributes to micro-vascular abnormalization and blood-retinal barrier breakdown in diabetic retinopathy. PLoS One 2011;6(3):e17462. [PubMed: 21408222]
22. Mitamura Y, Tashimo A, Nakamura Y, Tagawa H, Ohtsuka K, Mizue Y, Nishihira J. Vitreous levels of placenta growth factor and vascular endothelial growth factor in patients with proliferative diabetic retinopathy. Diabetes Care 2002;25(12):2352. [PubMed: 12453985]

23. Van Bergen T, Hu TT, Etienne I, Reyns GE, Moons L, Feyen JHM. Neutralization of placental growth factor as a novel treatment option in diabetic retinopathy. Exp Eye Res 2017;165:136–150. [PubMed: 28965804]
24. Huang H, Shen J, Vinores SA. Blockade of VEGFR1 and 2 suppresses pathological angiogenesis and vascular leakage in the eye. PLoS One 2011;6(6):e21411. [PubMed: 21731737]
25. Huang H, Parlier R, Shen JK, Lutty GA, Vinores SA. VEGF receptor blockade markedly reduces retinal microglia/macrophage infiltration into laser-induced CNV. PLoS One 2013;8(8):e71808. [PubMed: 23977149]
26. Al Kahtani E, Xu Z, Al Rashaed S, Wu L, Mahale A, Tian J, Abboud EB, Ghazi NG, Kozak I, Gupta V and others. Vitreous levels of placental growth factor correlate with activity of proliferative diabetic retinopathy and are not influenced by bevacizumab treatment. Eye (Lond) 2017;31(4):529–536. [PubMed: 27886182]
27. Khaliq A, Foreman D, Ahmed A, Weich H, Gregor Z, McLeod D, Boulton M. Increased expression of placenta growth factor in proliferative diabetic retinopathy. Lab Invest 1998;78(1):109–16. [PubMed: 9461127]
28. Diabetic Retinopathy Clinical Research N, Wells JA, Glassman AR, Ayala AR, Jampol LM, Aiello LP, Antoszyk AN, Arnold-Bush B, Baker CW, Bressler NM and others. Aflibercept, bevacizumab, or ranibizumab for diabetic macular edema. N Engl J Med 2015;372(13):1193–203. [PubMed: 25692915]
29. Fagiani E, Christofori G. Angiopoietins in angiogenesis. Cancer letters 2013;328(1):18–26. [PubMed: 22922303]
30. Fukuhara S, Sako K, Noda K, Zhang J, Minami M, Mochizuki N. Angiopoietin-1Tie2 receptor signaling in vascular quiescence and angiogenesis. Histology and histopathology 2010.
31. Fiedler U, Scharpfenecker M, Koidl S, Hegen A, Grunow V, Schmidt JM, Kriz W, Thurston G, Augustin HG. The Tie-2 ligand angiopoietin-2 is stored in and rapidly released upon stimulation from endothelial cell Weibel-Palade bodies. Blood 2004;103(11):4150–4156. [PubMed: 14976056]
32. Hammes HP, Lin J, Wagner P, Feng Y, Vom Hagen F, Krzizok T, Renner O, Breier G, Brownlee M, Deutsch U. Angiopoietin-2 causes pericyte dropout in the normal retina: evidence for involvement in diabetic retinopathy. Diabetes 2004;53(4):1104–10. [PubMed: 15047628]
33. Rangasamy S, Srinivasan R, Maestas J, McGuire PG, Das A. A potential role for angiopoietin 2 in the regulation of the blood-retinal barrier in diabetic retinopathy. Invest Ophthalmol Vis Sci 2011;52(6):3784–91. [PubMed: 21310918]
34. Khalaf N, Helmy H, Labib H, Fahmy I, El Hamid MA, Moemen L. Role of Angiopoietins and Tie-2 in Diabetic Retinopathy. Electron Physician 2017;9(8):5031–5035. [PubMed: 28979738]
35. Wimmer RA, Leopoldi A, Aichinger M, Wick N, Hantusch B, Novatchkova M, Taubenschmid J, Hammerle M, Esk C, Bagley JA and others. Human blood vessel organoids as a model of diabetic vasculopathy. Nature 2019;565(7740):505–510. [PubMed: 30651639]
36. Huang H, Lennikov A, Saddala MS, Gozal D, Grab DJ, Khalyfa A, Fan L. Placental growth factor negatively regulates retinal endothelial cell barrier function through suppression of glucose-6-phosphate dehydrogenase and antioxidant defense systems. FASEB J 2019;33(12):13695–13709. [PubMed: 31585507]
37. Lennikov A, Mukwaya A, Fan L, Saddala MS, De Falco S, Huang H. Synergistic interactions of PlGF and VEGF contribute to blood-retinal barrier breakdown through canonical NFkappaB activation. Exp Cell Res 2020;397(2):112347. [PubMed: 33130176]
38. Van de Veire S, Stalmans I, Heindryckx F, Oura H, Tijeras-Raballand A, Schmidt T, Loges S, Albrecht I, Jonckx B, Vinckier S and others. Further pharmacological and genetic evidence for the efficacy of PlGF inhibition in cancer and eye disease. Cell 2010;141(1):178–90. [PubMed: 20371353]
39. Wimmer RA, Leopoldi A, Aichinger M, Kerjaschki D, Penninger JM. Generation of blood vessel organoids from human pluripotent stem cells. Nat Protoc 2019;14(11):3082–3100. [PubMed: 31554955]
40. Giaever I, Keese CR. Micromotion of mammalian cells measured electrically. Proc Natl Acad Sci U S A 1991;88(17):7896–900. [PubMed: 1881923]

41. Huang H, Van de Veire S, Dalal M, Parlier R, Semba RD, Carmeliet P, Vinores SA. Reduced retinal neovascularization, vascular permeability, and apoptosis in ischemic retinopathy in the absence of prolyl hydroxylase-1 due to the prevention of hyperoxia-induced vascular obliteration. Invest Ophthalmol Vis Sci 2011;52(10):7565–73. [PubMed: 21873682]
42. Saddala MS, Lennikov A, Mukwaya A, Yang Y, Hill MA, Lagali N, Huang H. Discovery of novel L-type voltage-gated calcium channel blockers and application for the prevention of inflammation and angiogenesis. J Neuroinflammation 2020;17(1):132. [PubMed: 32334630]
43. Saddala MS, Lennikov A, Mukwaya A, Huang H. Transcriptome-Wide Analysis of CXCR5 Deficient Retinal Pigment Epithelial (RPE) Cells Reveals Molecular Signatures of RPE Homeostasis. Biomedicines 2020;8(6).
44. Verbeke G, Molenberghs G. Linear Mixed Models for Longitudinal Data. New York: Springer-Verlag, Inc; 2000.
45. Sweeney M, Foldes G. It Takes Two: Endothelial-Perivascular Cell Cross-Talk in Vascular Development and Disease. Front Cardiovasc Med 2018;5:154. [PubMed: 30425990]
46. Teichert M, Milde L, Holm A, Stanicek L, Gengenbacher N, Savant S, Ruckdeschel T, Hasanov Z, Srivastava K, Hu J and others. Pericyte-expressed Tie2 controls angiogenesis and vessel maturation. Nat Commun 2017;8:16106. [PubMed: 28719590]
47. Huang H. Pericyte-Endothelial Interactions in the Retinal Microvasculature. Int J Mol Sci 2020;21(19).
48. Milam KE, Parikh SM. The angiopoietin-Tie2 signaling axis in the vascular leakage of systemic inflammation. Tissue Barriers 2015;3(1-2):e957508. [PubMed: 25838975]
49. Piera-Velazquez S, Jimenez SA. Endothelial to Mesenchymal Transition: Role in Physiology and in the Pathogenesis of Human Diseases. Physiol Rev 2019;99(2):1281–1324. [PubMed: 30864875]
50. Bischoff J. Endothelial-to-Mesenchymal Transition. Circ Res 2019;124(8):1163–1165. [PubMed: 30973806]
51. Wheelock MJ, Shintani Y, Maeda M, Fukumoto Y, Johnson KR. Cadherin switching. J Cell Sci 2008;121(Pt 6):727–35. [PubMed: 18322269]
52. Saddala MS, Lennikov A, Mukwaya A, Yang X, Tang S, Huang H. Data mining and network analysis reveals C-X-C chemokine receptor type 5 is involved in the pathophysiology of age-related macular degeneration. J Biomol Struct Dyn 2021:1–10.
53. Xu X, Yan Y, Xun Q, Shi J, Kong X, Wu J, Zhou H. Combined silencing of VEGF-A and angiopoietin-2, a more effective way to inhibit the Ishikawa endometrial cancer cell line. Onco Targets Ther 2019;12:1215–1223. [PubMed: 30863089]
54. Khanani AM, Russell MW, Aziz AA, Danzig CJ, Weng CY, Eichenbaum DA, Singh RP. Angiopoietins as Potential Targets in Management of Retinal Disease. Clin Ophthalmol 2021;15:3747–3755. [PubMed: 34511878]
55. Akwii RG, Mikelis CM. Targeting the Angiopoietin/Tie Pathway: Prospects for Treatment of Retinal and Respiratory Disorders. Drugs 2021;81(15):1731–1749. [PubMed: 34586603]
56. Whitehead M, Osborne A, Widdowson PS, Yu-Wai-Man P, Martin KR. Angiopoietins in Diabetic Retinopathy: Current Understanding and Therapeutic Potential. J Diabetes Res 2019;2019:5140521. [PubMed: 31485452]
57. Shirley M Faricimab: First Approval. Drugs 2022;82(7):825–830. [PubMed: 35474059]
58. Striglia E, Caccioppo A, Castellino N, Reibaldi M, Porta M. Emerging drugs for the treatment of diabetic retinopathy. Expert Opin Emerg Drugs 2020;25(3):261–271. [PubMed: 32715794]
59. Cai J, Kehoe O, Smith GM, Hykin P, Boulton ME. The angiopoietin/Tie-2 system regulates pericyte survival and recruitment in diabetic retinopathy. Invest Ophthalmol Vis Sci 2008;49(5):2163–71. [PubMed: 18436850]

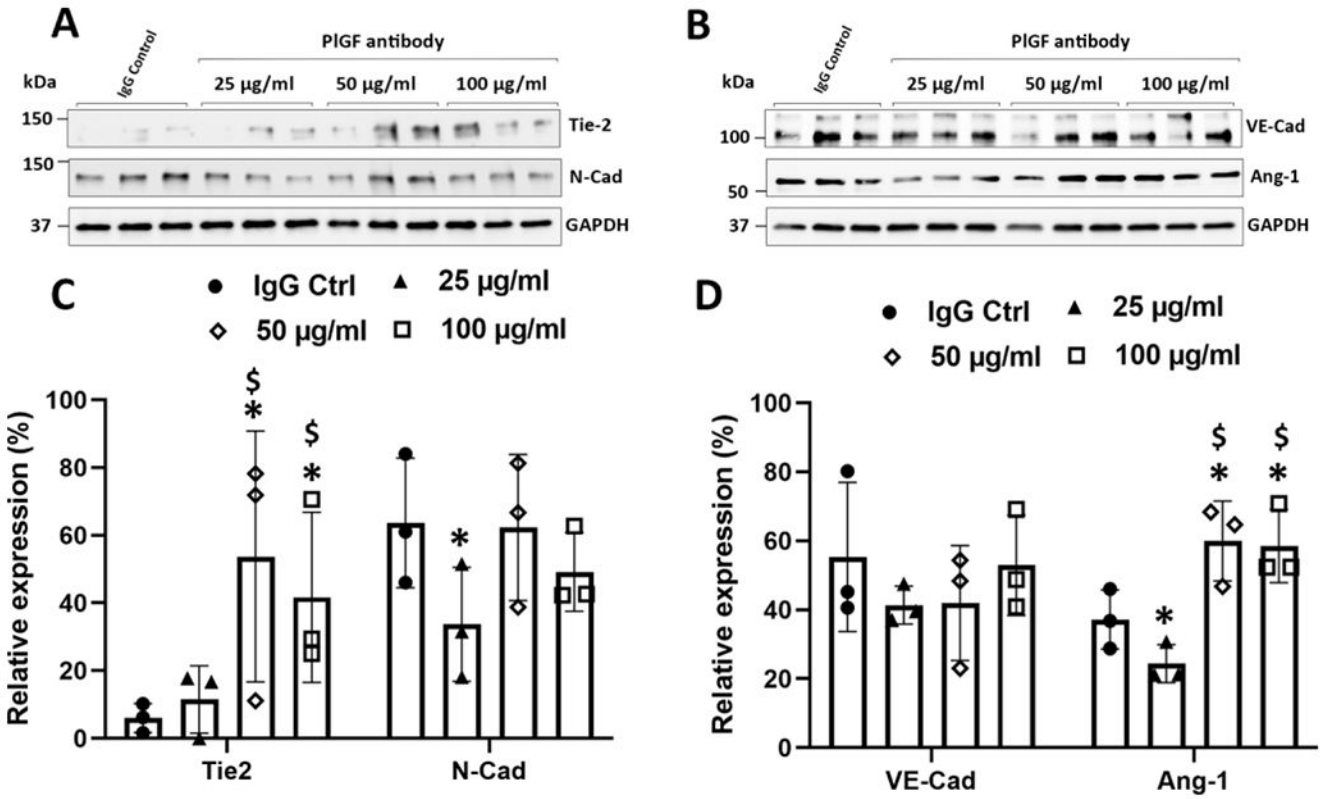

Figure 1. P*l*GF blockade regulates Ang-1 and Tie-2 protein expressions in HRP-HREC co-culture in an antibody dose-dependent manner.

Primary human retinal endothelial cells (HREC) and pericytes (HRP) are co-cultured at a 2:1 ratio. The confluent HRP-HREC co-cultures were treated with three P*l*GF antibody concentrations (25, 50, and 100 μg/ml) for two days. IgG was used as treatment control. (**A, B**) Western blotting results of Tie-2, N-Cadherin (N-Cad), VE-Cadherin (VE-Cad), and Angiopoietin-1 (Ang-1). GAPDH acted as a loading control. Note that the HREC-HRP co-cultures were used for all western blotting analyses. (**C, D**) Densitometry quantification results of the western blots. * indicates $P < 0.05$ compared with control. $ indicates $P < 0.05$ compared with 25μg/ml. It should be noted: that although the Tie-2 and Ang-1 WB results had variations among the three samples of 100 μg/ml P*l*GF antibody, the pixel intensities detected by Image J software were greater than any of the three controls, and thereby the ANOVA analysis leads to a statistically significant result ($p = 0.0408$ for Ang-1; $p = 0.0113$ for Ang-1).

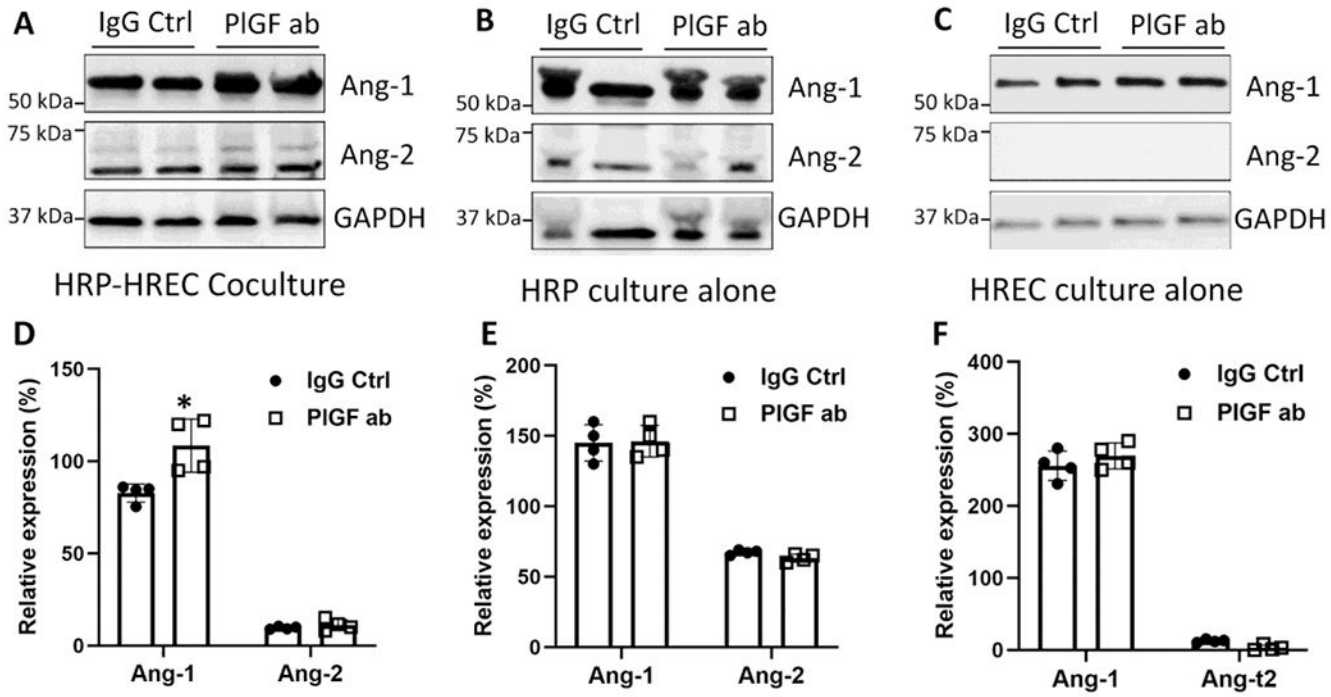

Figure 2. Ang-1 upregulation caused by P*l*GF blockade requires HRP-HREC co-culture.

Primary human retinal endothelial cells (HREC) and pericytes (HRP) are cultured alone or co-cultured as described in the methods. IgG and P*l*GF antibodies (50 μg/ml) treated the confluent co-culture and monoculture for two days. Western blots (WB) and densitometry analysis were performed to determine the protein expression. WB results of HRP-HREC coculture (**A**), HRP monoculture (**B**), and HREC monoculture (**C**). Densitometry quantification results of HRP-HREC co-culture (**D**), HRP monoculture (**E**), and HREC monoculture (**F**). * indicates $P < 0.05$ compared with IgG control.

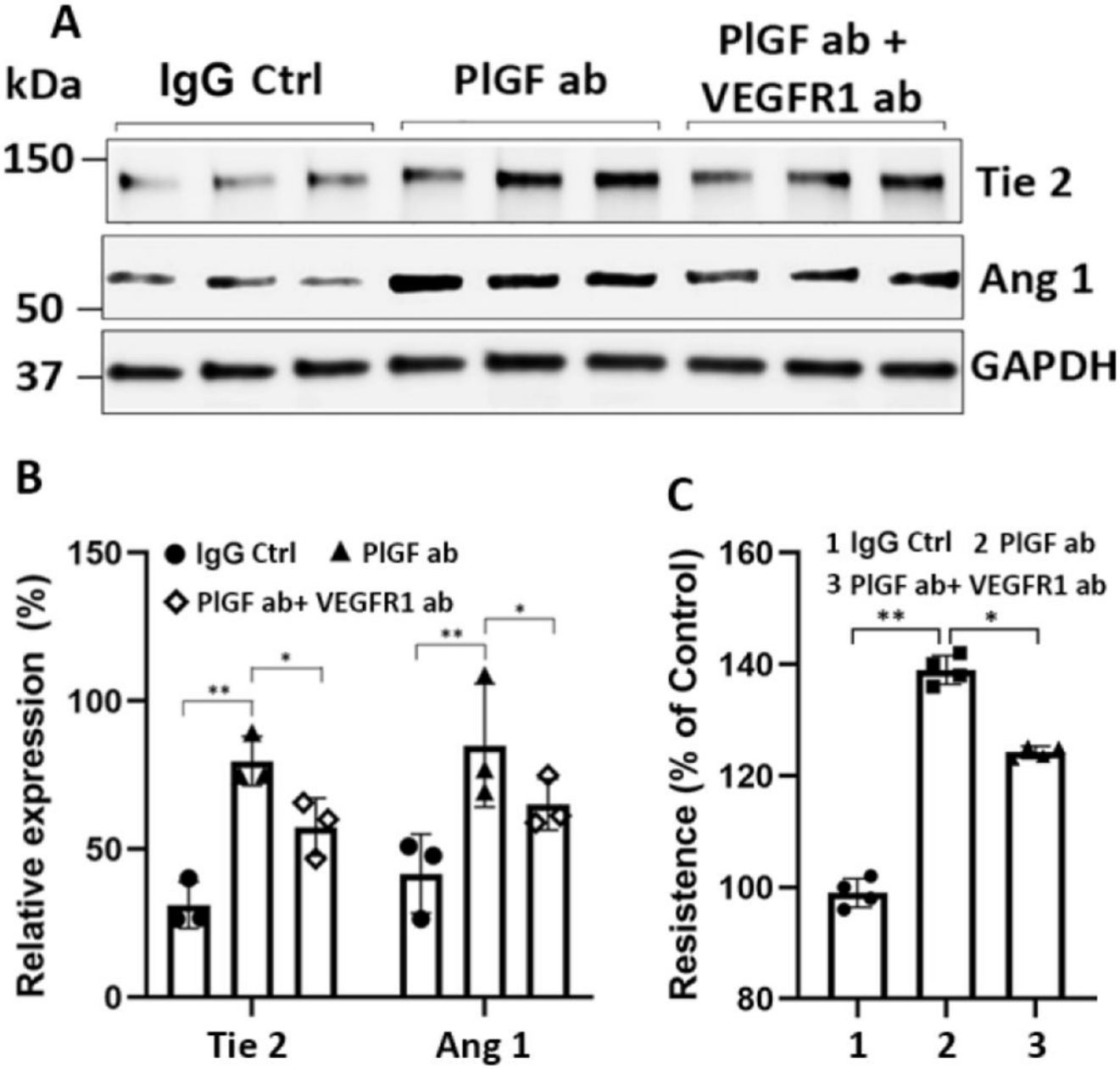

Figure 3. VEGFR1 inhibition diminishes P*l*GF's effect on Ang-1 and Tie-2 expression in the HREC-HRP co-culture.

HREC and HRP were co-cultured and treated with three groups: IgG control, PlGF antibody (ab) (50 μg/ml), and P*l*GF ab (50 μg/ml) + VEGFR1 ab (50 μg/ml). The western blots (**A**) and densitometry quantification results (**B**). GAPDH was used as a protein loading control. (**C**) Resistance results were measured with the ECIS system. The results were expressed as a percentage relative to the control (mean ± SD, n = 3 for WB, n = 4 for resistance). *P < 0.05. ** P < 0.01.

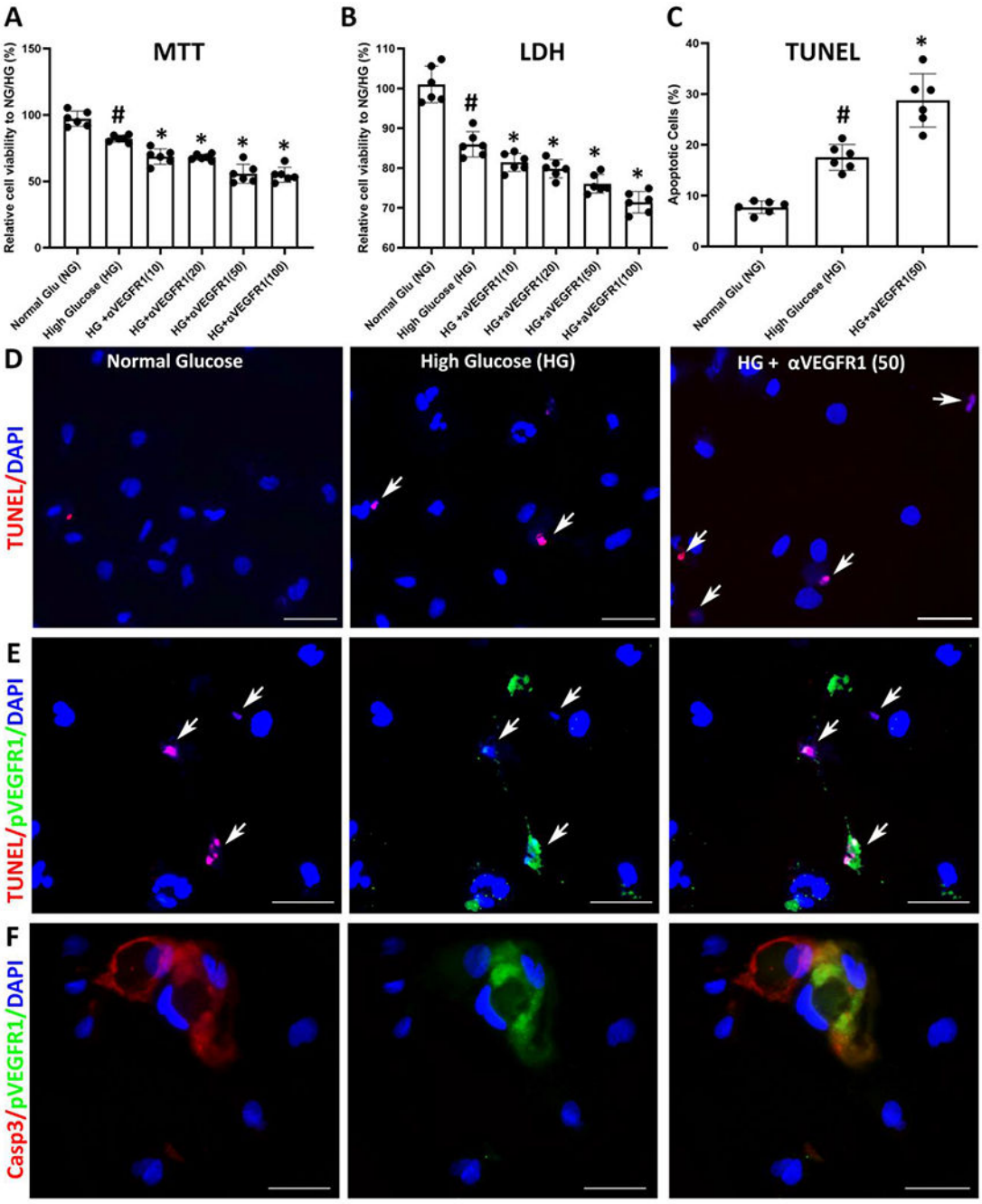

Figure 4. VEGFR1 inhibition reduces pericyte viability in high-glucose conditions.

The pericytes were cultured with normal glucose (NG), high glucose (HG), and HG + varying VEGFR1 antibody concentrations (10, 20, 50, and 100 μg/ml). The cell lysates were used for cell viability assay with MTT (**A**) and the supernatant for LDH assay (**B**). The results expressed relative cell viability to NG (mean ±SD, n=6). (**C and D**) The TUNEL (+) apoptotic cells were counted for NG, HG, and HG + 50 μg/ml VEGFR1 antibody. # $P < 0.05$ (compared to normal glucose). * $P < 0.05$ (compared to high glucose). (**E, F**) Double immunofluorescent labeling was performed for: pVEGFR1 and TUNEL (**E**),

activated Caspase 3 (a-Casp3), and pVEGFR1 (**F**). Scale bar: 50 μm. Note that pVEGFR1 staining signals were co-localized with the TUNEL(+) and a-Casp3 (+) apoptotic cells. The colocalization of TUNEL and DAPI was demonstrated with individual channels in Fig. S4.

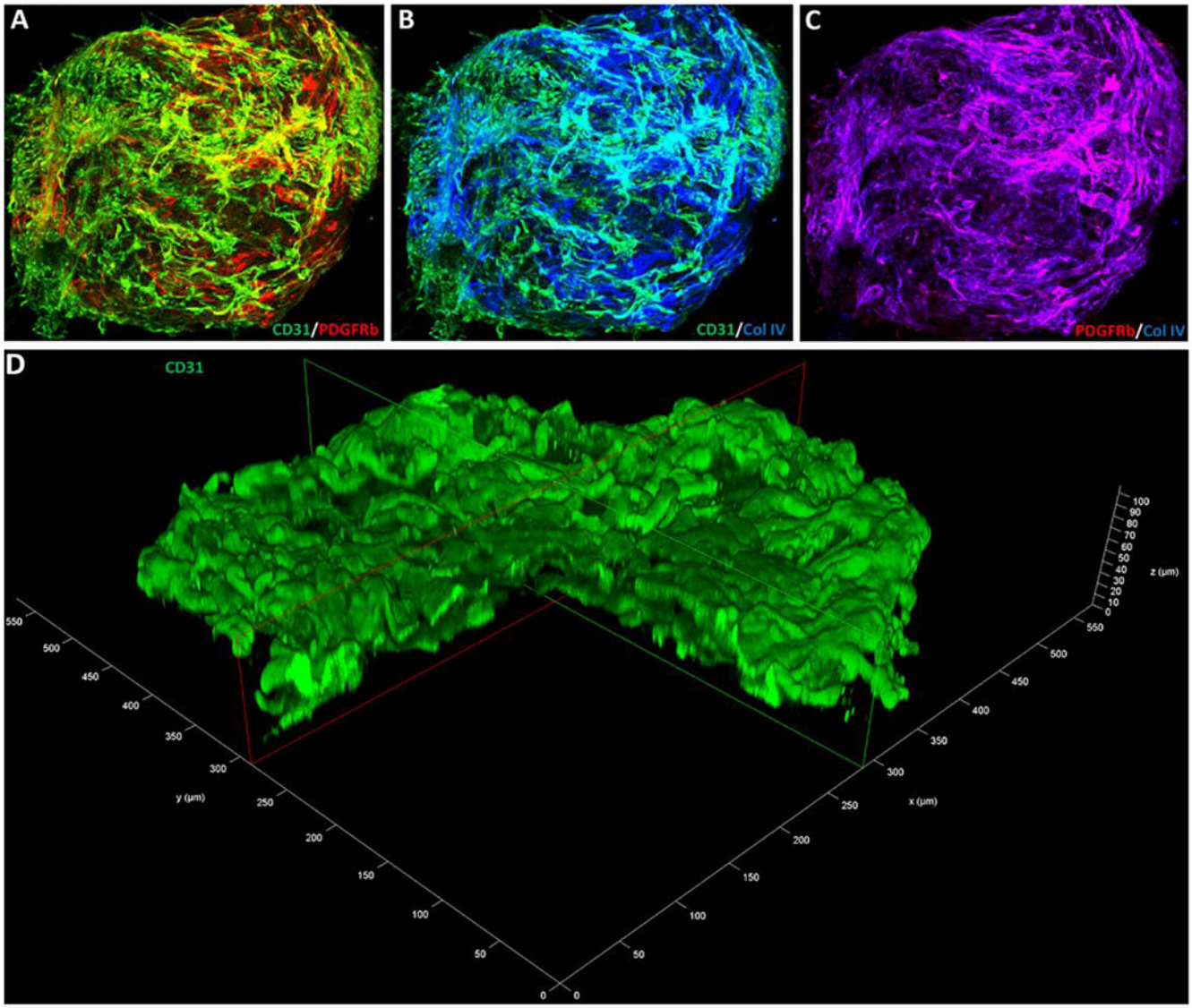

Fig 5. Blood vessels of vascular organoids.

Vascular organoids were generated from human induced pluripotent stem cells (iPSC). (A-C) The 3-dimensional (3D) vascular organoids were whole-mounted for the immunofluorescent staining with endothelial cell marker CD31, pericyte marker PDGFRb, and basement marker Collagen IV. The corresponding secondary antibodies conjugated with Cy5 (PDGFRb), Alexa fluor 488 (CD31), and pacific blue (Col IV) were used for the visualization and imaging with confocal microscopy. (D) illustrated the three dimensions of one vascular organoid (~500 μm x 500 μm x 100 μm).

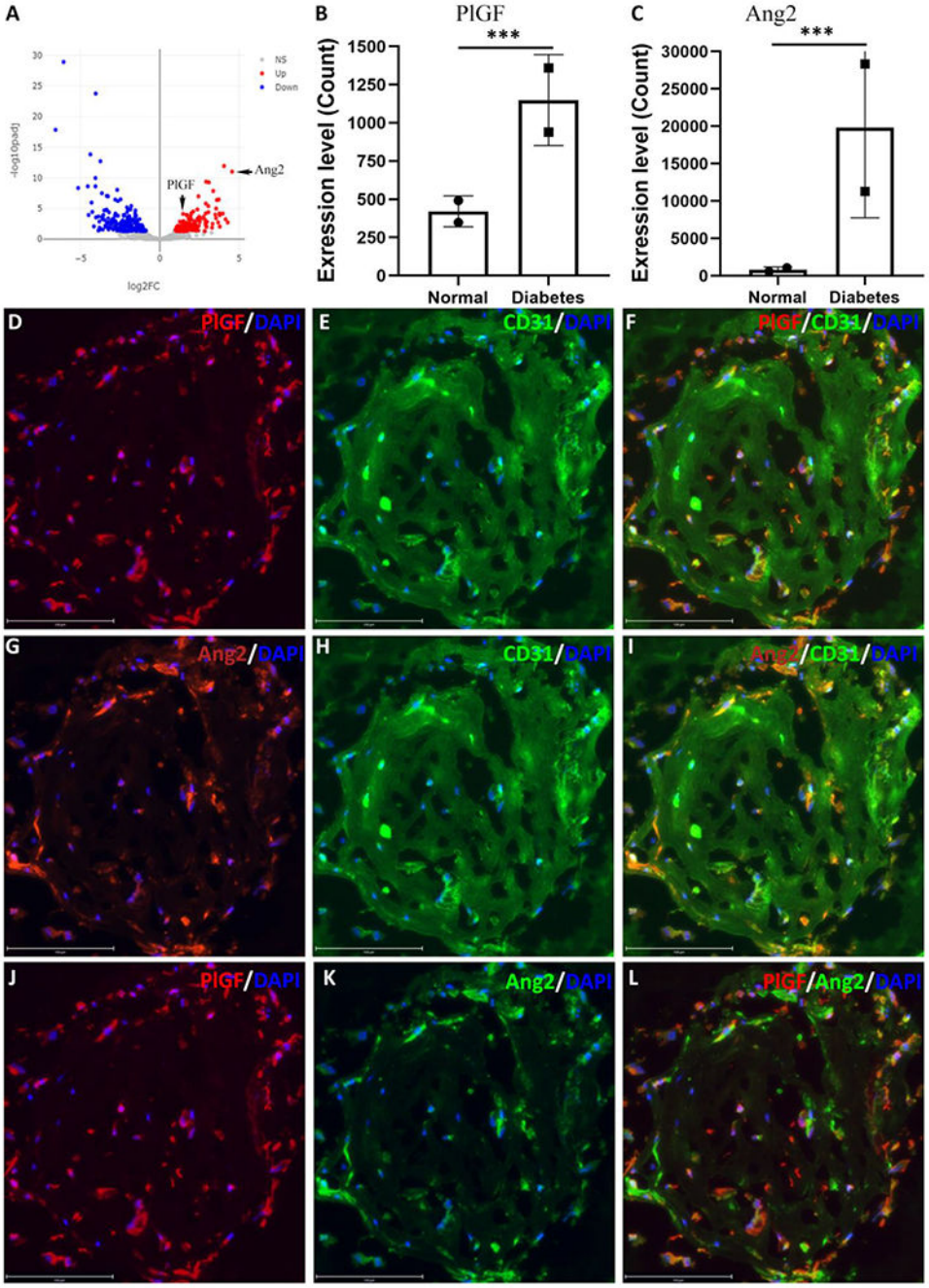

Figure 6. P*l*GF is expressed in perivascular (pericyte) cells and up-regulated by diabetes-mimicking conditions in the human iPSC-derived vascular organoids.

(**A-C**) Bioinformatic RNA sequencing analysis revealed that diabetes-mimicking conditions up-regulated PlGF and Ang2. Volcano plot (**A**) showed the differentially expressed genes between normal and diabetic conditions, in which arrows indicated P*l*GF and Ang2. Their expression levels were shown in P*l*GF (**B**) and Ang2 (**C**). *** $P < 0.0001$.(**D-L**) Double labeling revealed PlGF and Ang2 had a perivascular (pericyte) localization in the human iPSC-derived vascular organoids. Scale bar: 150 μm.

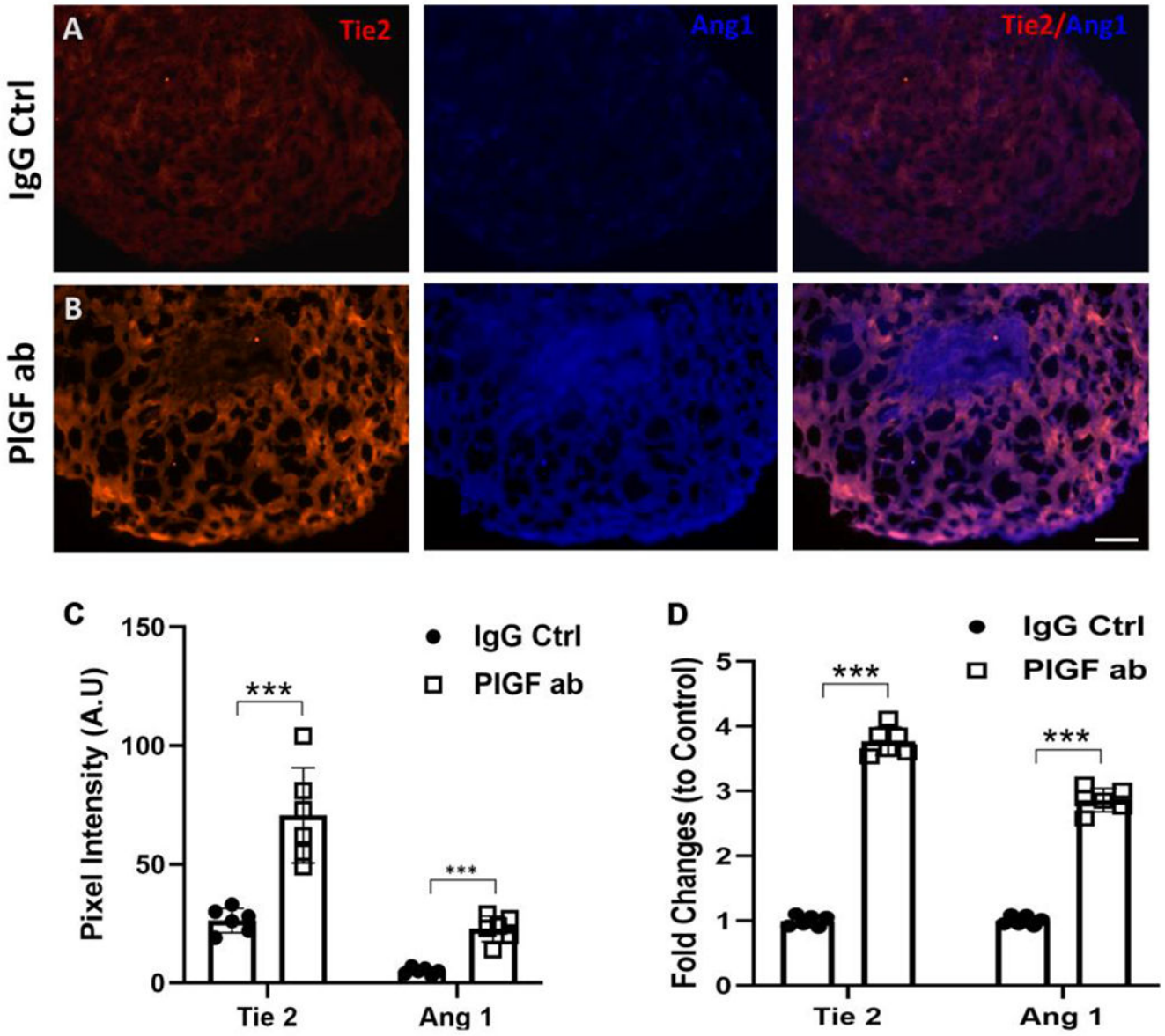

Figure 7. P*l*GF blockade up-regulates Ang-1 and Tie-2 in human iPSC-derived vascular organoids.

Vascular organoids were generated from human iPSC as described in the methods. 100 μg/ml P*l*GF antibody was supplemented into the culture medium and incubated for 4 days. IgG was used as a control. 10-micron cryopreserved sections were made for immunofluorescent staining with anti-Ang-1 and anti-Tie-2 antibodies. The secondary antibodies with Alex Fluor 647 (infrared) and 488 (green) were used for visualization and microphotography with EVOS M7000 fluorescent microscope (**A, B**). Scale bar: 75 μm. (**C**) Quantification results of the fluorescent images measured with ImageJ software (n = 6). *** $P < 0.0001$. The fluorescent images from each channel were made with the same exposure time for both control and antibody treatment conditions to minimize the variations caused by the fluorescent imaging process. The expression levels were measured based on the mean pixel intensity per image (6 images total). The two additional example images

used for quantification were shown in Suppl. Fig. 4. Note that Ang-1 had a peri-vascular (pericyte) expression pattern similar to P*l*GF and Ang2. (**D**) qRT-PCR results of Tie-2 and Ang-1 mRNA transcripts. The values represent the change folds relative to the control (n = 6). *** $P < 0.0001$.

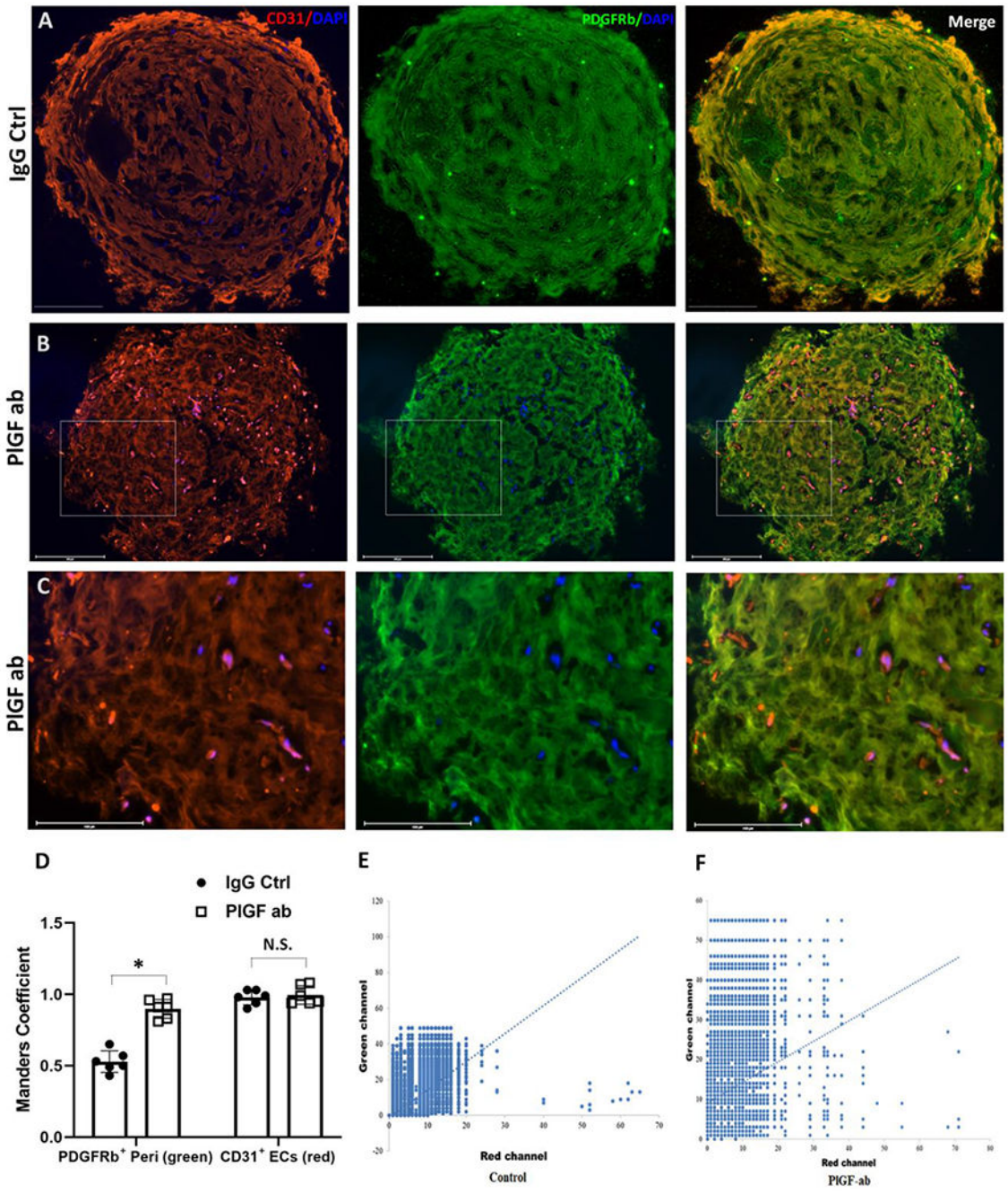

Figure 8. P*l*GF blockade promotes the pericytes coverage and association with ECs in vascular organoids.

Vascular organoids (VO) were derived from human iPSC derived. The VO micrographs double-stained with CD31 (red channel) and PDGFRb (green channel) were processed for colocalization analysis with Image J software and the JACop plugin. (**A and B**) The micrographs were from the control group (**A**) and P*l*GF antibody treatment (**B**). Scale bar: 275 μm. (**C**) The box areas in Panel B showed the colocalization of CD31 (red) and PDGFRb (green). Scale bar: 150 μm. (**D**) The Manders' overlay coefficients indicate the

degree of colocation: M1 stands for the green ($PDGFRb^+$ pericytes), and M2 for the red ($CD31^+$ EC). The values were expressed as mean percentage ± SD (n = 6). * Indicates $p < 0.05$. N.S: Non-Significance. (**E and F**) Cytofluorogram showed the Pearson correlation coefficients between the green and red channels (E: IgG control; F: PlGF ab).

Table 1:

A list of primary antibodies and dilutions used in the western blotting and immunofluorescent staning

Target protein	Produced by	Catalog number	Host	WB dilution	IHC dilution
Ang-1	Abclonal	A7877	Rabbit	1:500	1:100
Ang-2	Abclonal	A0698	Rabbit	1:500	1:100
Tie-2	Abcam	ab24859	Mouse	1:500	1:100
VE-cadherin	Thermo Fisher Scientific	50-128-96	Mouse	1:1000	N/A
N-cadherin	Thermo Fisher Scientific	33-390-0	Mouse	1:1000	N/A
GAPDH	Sigma	G9545	Rabbit	1:1000	N/A
CD31	Biolegend	375902	Rat		1:100
Cleaved Caspase-3	Cell Signalling	Asp175	Rabbit	N/A	1:100
Phospho-VEGFR1	R&D Systems	Y1213	Rabbit	N/A	1:50
PDGFRb	Cell Signaling	3169S	Rabbit	N/A	1:100
Collagen IV	Invitrogen	MA1-22148	Mouse	N/A	1:100

Table 2:

A list of mouse-specific primers used in the study

Gene	Forward/Reverse	Primer sequence	Reference sequence
Ang-1	Forward	5′-AGAAGGTGTTTTACTAAAGGGAGG -3′	BC152419.1
	Reverse	5′-CAGTCCAACCTCCCCCATTG-3′;	
Tie-2	Forward	5′-GTTCTGTCTCCCTGACCCCT-3′	BC035514.1
	Reverse	5′-TGGAAGCGATCACACATCTCC-3′;	
Cyclophilin	Forward	5′- CAGACGCCAC-TGTCGCTTT -3′	N/A
	Reverse	5′- TGTCTTTGGAACTTTGTCTG -3′;	